Optics and Lasers in Engineering 46 (2008) 671–678

Contents lists available at ScienceDirect

Optics and Lasers in Engineering

journal homepage: www.elsevier.com/locate/optlaseng

Optimisation of TA6V alloy surface laser texturing using an experimental design approach

A. Soveja [a,b,*], E. Cicală [b], D. Grevey [a], J.M. Jouvard [a]

[a] Département Interface et Réactivité des Matériaux, Institut Carnot de Bourgogne, UMR CNRS 5209, Université de Bourgogne, IUT Le Creusot, 12 rue de la Fonderie, 71200 Le Creusot, France
[b] Faculté de Génie Mécanique, Université "Politehnica" Timişoara, P-ta Victorei, Nr 2, 300006 Timisoara, Romania

ARTICLE INFO

Article history:
Received 21 January 2008
Received in revised form
28 March 2008
Accepted 7 April 2008
Available online 2 June 2008

Keywords:
Laser texturing
Titanium alloy
Experimental design
Parameters optimisation

ABSTRACT

Active surfaces of plastic injection moulds are nowadays textured using classical techniques (chemical etching or EDM). Replacement of these technologies by a laser technology introduces a big flexibility: absence of mechanical contact with the tool, decrease of the effluent's volume and a big machining precision, even in the case of the complex forms as injection moulds for example. This paper reports the experimental study of the surface laser texturing of TA6V alloy. The influence of the operating factors on the laser texturing process has been studied using two experimental approaches: Taguchi methodology and response surface methodology (RSM). Empirical models have been developed. They allowed us to determine a correlation between process operating factors and performance indicators, such as surface roughness and material removal rate. Results analysis shows that the laser pulse energy and frequency are the most important operating factors. Mathematical models, that have been developed, can be used for the selection of operating factors' proper values in order to obtain the desired values of the objective functions.

1. Introduction

One of the basic quality criteria, for plastic ornamental car body, is the first visual impression. Consequently, almost all injection moulds, used for this purpose, are provided with textured active surfaces. Texturing process means manufacturing micro/macro geometrical patterns on metallic surface using different methods. There are a lot of surface texturing processes, each of them having its own limits. So, performance indicators like surface quality, productivity or manufacturing price reduction are important reasons to choose a laser process over other texturing techniques (chemical etching or EDM).

Using a laser method allows one to eliminate some inconveniences like environment chemical pollution or limitations of the treated material. Knowing that laser texturing is a complex process, it is necessary to identify the operating parameters having a significant influence on the performance indicators [1]. Looking for an improvement in the laser machining process, a lot of researches [2–8] on various materials have been carried out in the last few years, in order to determine the effects of the operating factors influencing the process. Using an experimental design, Lallemand et al. [9] analysed the influence of operating parameters on the geometry and quality of grooving. Li et al. [10] showed that the morphology of the crater obtained by laser texturing technology is mainly influenced by electrical polarity of laser beam and work medium. Other studies [11–13] have proved that pulse frequency has a significant influence on the laser-machined surface roughness. A lot of research has been conducted in the domain of laser surface texturing in order to improve the tribological properties (lubrication, fretting coefficient, etc.) of surfaces [14–17], but none of them presents a clear correlation between performance indicators and influencing factors.

One of the problems that is not yet resolved is to establish a correlation between productivity and surface quality in order to allow laser texturing process to be implemented in industrial manufacturing process of injection moulds. Consequently, the aim of this study is to obtain the biggest possible productivity for a surface roughness smaller than 5 μm. An experimental design approach has been used to study the limitations of laser surface texturing of TA6V alloy and the most influencing operating factors are pointed out, concerning both productivity and surface quality in order to optimise the process. In this research, the metallurgical changes of surface are not studied.

* Corresponding author at: Département Interface et Réactivité des Matériaux, Institut Carnot de Bourgogne, UMR CNRS 5209, Université de Bourgogne, IUT Le Creusot, 12 rue de la Fonderie, 71200 Le Creusot, France. Tel.: +33 3 85 73 10 56; fax: +33 3 85 73 11 20.
E-mail address: adriana.soveja@u-bourgogne.fr (A. Soveja).

0143-8166/$ - see front matter © 2008 Elsevier Ltd. All rights reserved.
doi:10.1016/j.optlaseng.2008.04.009

2. Experimental set-up

A Q-switch Nd:YAG laser equipped with a galvanometric head was used (Fig. 1) in the experiments. A diaphragm of 4 mm diameter was put into the laser cavity between the back mirror and the rod to improve the quality of the beam. The operating characteristics of laser beam are presented in Table 1.

The experiments were carried out on TA6V alloy (Table 2) sheets, all of them having the same geometry (Fig. 2a). A pattern (Fig. 2b) was machined on the specimen surface by sweeping the laser beam. In order to gain an easily characterised print, sweeping was performed six times with alternate passes at 0° and 90°. Each specimen was weighed before and after machining, and the machining time was measured. In that way, the machining rates can be calculated.

The common laser experimental conditions in all tests were as follows:

- laser beam wavelength 1.06 μm;
- laser beam was delivered through a diaphragm with 4 mm in diameter; and
- laser spot diameter was 320 μm on the surface of the specimens, with normal incidence. It was considered that the spot diameter remains unchangeable during texturing process. This choice was taken knowing that the near field of focus lens is big enough for the machined depth of texture.

After machining, the surface roughness of specimens was measured with an InfiniteFocus optical microscope. It is an optical device for 3D surface measurements. Its operating principle combines the small depth of focus of an optical system with vertical scanning to provide topographical information from the variation of focus. It allows having a "Z" resolution as low as 20 nm.

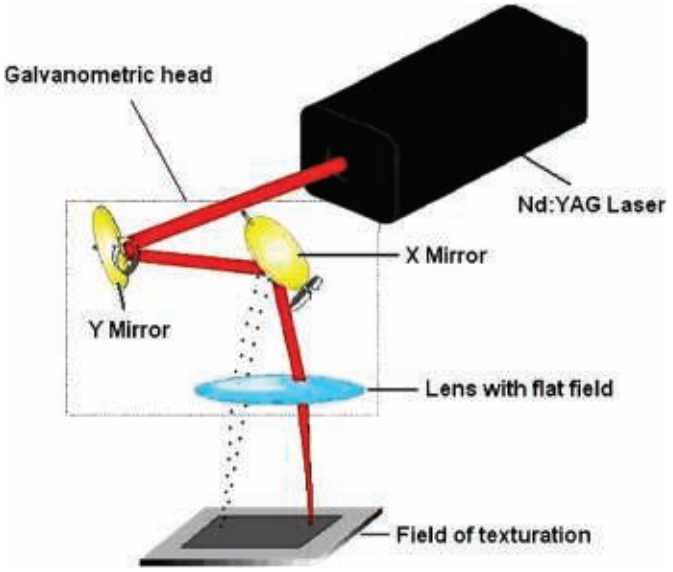

Fig. 1. Schematic representation of laser texturing system (Rofin courtesy).

Table 1
Laser beam characteristics

Wavelength λ (nm)	1064
Focused spot diameter d (μm)	320
Maximum average power P_{av} (W)	70
Maximum peak power P_p (kW)	61
Pulse energy E (mJ)	0,2–11
Pulse width t_p (ns)	150–780
Frequency f (kHz)	1–30

3. Experimental results and discussions

Due to the poor knowledge on laser parameters' influence on the productivity and surface quality in surface texturing, the tests were carried out using a modern experimental strategy [18–21]. This strategy consists in performing a number of tests that enable a determination of parameters which have a significant influence on the process and determination of the optimal work domain. In order to achieve this, the research was conducted by the following steps:

- identification of the factors that have a significant influence on the objective functions;
- development of an experimental design matrix in order to obtain a mathematical model of objective functions variation vs. factors influence;
- development of the mathematical model and verification of its adequacy; and
- analysis of the effects of different influence factors on the objective functions in order to find the optimal working range.

3.1. Influencing factors identification using Taguchi method

We began our researches by determining the hierarchy of laser parameters in sense of the significance of their influence on productivity and surface quality. This study was carried out using Taguchi method. The Taguchi design method is a simple and powerful technique used to identify significant factors. In this method, parameters which are assumed to influence performance

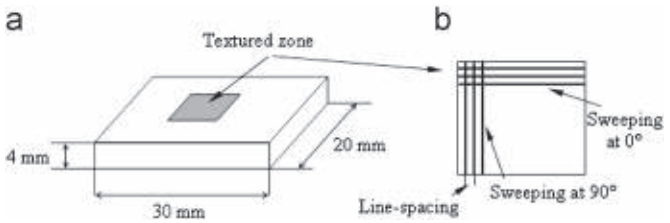

Fig. 2. The specimens' geometry (a) and laser machined cross sweeping (b).

Table 2
Chemical composition of TA6V alloy

Material	Weight (%)						
TA6V	Al 5.5–6.75	V 3.5–4.5	O 0.2 (maximum)	Fe 0.4 (maximum)	H 0.015 (maximum)	C 0.1 (maximum)	N 0.05 (maximum)

indicators are located at different levels in a designed orthogonal matrix.

The studied objective functions are as follows.

(1) Material removal rate, MRR ($mm^3\,min^{-1}$):

$$\mathrm{MRR} = \frac{\Delta m}{\rho t}, \tag{1}$$

where Δm is the quantity of removed matter (mg), ρ is the material density ($mg\,mm^{-3}$) and t is the machining time (min).

(2) Surface roughness, S_a (μm), which is used to analyse the surface aspect in 3D orientation and is given by following equation:

$$S_a = \frac{1}{a}\int\int_a |Z(x,y)|\,dx\,dy, \tag{2}$$

where a is the analysed surface area (mm^2) and Z is the peak-valley value in x and y orientations.

(3) Composite function, C_f ($mm^2\,min^{-1}$):

$$C_f = \frac{\mathrm{MRR}}{S_a}. \tag{3}$$

Based on data from the literature and some previous tests performed by the authors, it was chosen to analyse the influence of the following four factors: pulse frequency (f), pulse energy (E), sweeping speed (s) and line spacing (l_s). The factors' levels and their physical values are presented in Table 3. In these conditions, the total number of required experiments was reduced to 16. The combinations of factors as well as observed values of objective functions are presented in Table 4. These results are used to calculate the generated effects on objective functions [18–20].

Results' analysis shows that the material removal rate increases with increasing pulse frequency and energy, but it decreases with decreasing sweeping speed (Fig. 3). It was observed that up to a certain value of line spacing, the material removal rate increases but after that value, it decreases. For a 95% confidence level (Fig. 3: dotted line), all influencing factors have a significant influence on the material removal rate. According to the results, the pulse frequency is the most important influencing factor, closely followed by the pulse energy. Sweeping speed and line spacing are situated on the third and fourth place of this importance hierarchy. The results show that the biggest material removal rate can be obtained by working at 9500 Hz frequency, 6 mJ energy, 6 mm s^{-1} sweeping speed and 70 μm line spacing.

The surface roughness is proportional to the pulse energy and decreases with increasing sweeping speed. On the other hand, no variation of the surface roughness is observed with a variation of the frequency (Fig. 4). The most influential factor is the pulse energy, followed by line spacing. In this case, the third and fourth places belong to sweeping speed and pulse frequency. In case of a 95% confidence level, only pulse energy has a significant influence on the surface roughness. Under these conditions, the minimal surface roughness was obtained using the lowest value of energy (3 mJ) and

Table 3
Experimental factors and their levels

Factor levels	Physical values			
	f (Hz)	E (mJ)	s (mm s^{-1})	l_s (μm)
1	3500	3	6	30
2	5500	4	9	50
3	7500	5	12	70
4	9500	6	15	90

Table 4
Taguchi design matrix and observed values of objective functions

Test no.	Influence factors coded values				Objectives functions		
	F	E	s	l_s	MRR ($mm^3\,min^{-1}$)	S_a (μm)	C_f ($mm^2\,min{-}1$)
1	1	1	1	1	0.70	47.93	14.60
2	1	2	2	2	0.80	47.28	16.92
3	1	3	3	3	1.07	52.46	20.40
4	1	4	4	4	1.11	49.41	22.47
5	2	1	2	4	0.87	31.25	27.84
6	2	2	1	3	2.09	39.63	52.74
7	2	3	4	2	1.45	55.43	26.16
8	2	4	3	1	1.72	70.76	24.31
9	3	1	3	2	1.06	32.95	32.17
10	3	2	4	1	1.51	36.71	41.13
11	3	3	1	4	1.94	52.21	37.16
12	3	4	2	3	2.39	49.35	48.43
13	4	1	4	3	1.47	20.23	72.66
14	4	2	3	4	1.75	15.11	115.82
15	4	3	2	1	2.16	36.67	58.90
16	4	4	1	2	2.74	158.6	17.28

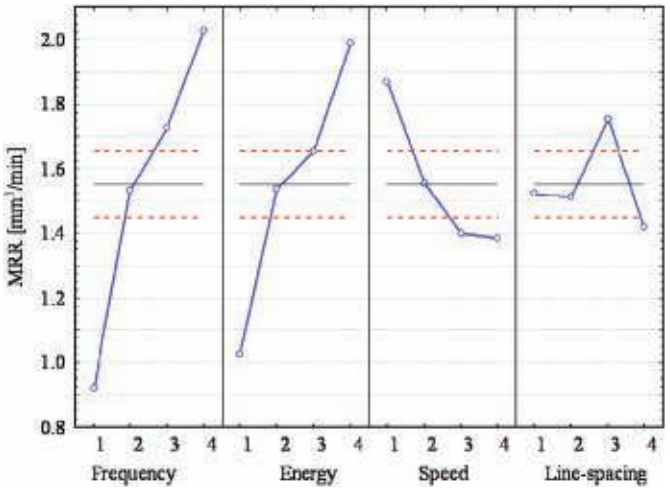

Fig. 3. Diagram of influencing factors generated effects on MRR.

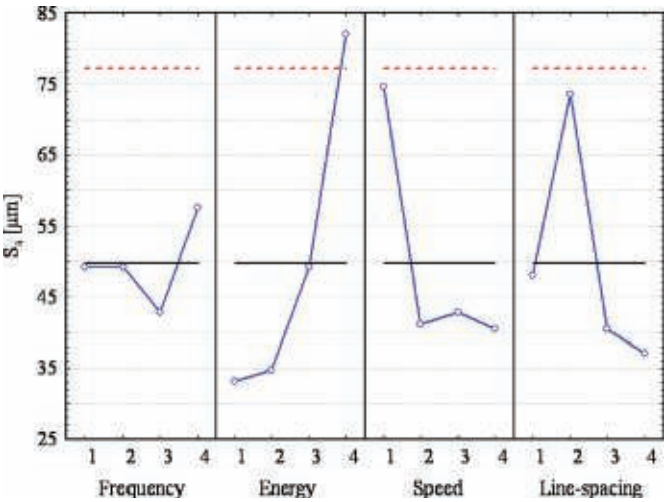

Fig. 4. Diagram of influencing factors generated effects on S_a.

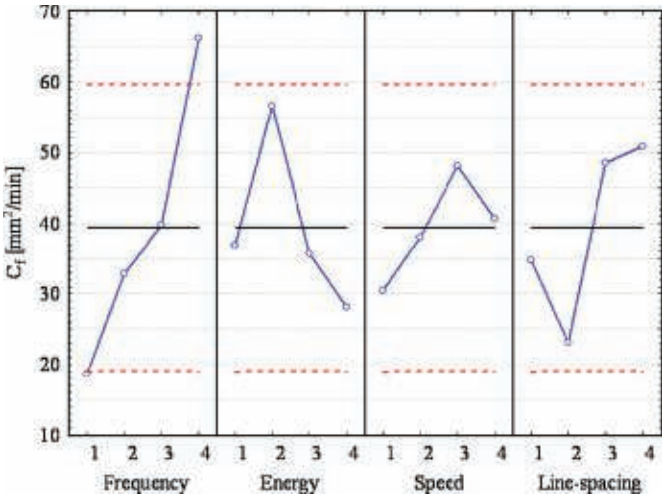

Fig. 5. Diagram of influencing factors generated effects on C_f.

a sweeping speed around 12 mm s^{-1} for an appropriate rate of superposition of pulses (big frequency and small line spacing).

Material removal rate and surface roughness are directly proportional to pulse energy and inversely proportional to sweeping speed. Hence, it is very difficult to find a combination of factors, which allows the maximising of the material removal rate and minimising of the surface roughness at the same time. So, it was decided to examine the influence of these factors on the composite function. The experimental results showed that the maximum of composite function is obtained for a 4 mJ pulse energy and 12 mm s^{-1} sweeping speed (Fig. 5). On the other hand, the composite function is directly proportional to frequency variation. The most influential factor in this case is pulse frequency, followed by pulse energy, line spacing and sweeping speed. For a 95% confidence level, only pulse frequency has a significant influence on the composite function.

After a detailed analysis of the first set of tests, it was chosen to retain two influencing factors due to their significant influence on three examined objective functions: the frequency and the pulse energy. In further tests, the sweeping speed and line spacing were maintained at a constant value, i.e. sweeping speed at 12 mm s^{-1} and line spacing, for practical reasons, at 30 μm.

3.2. Mathematical modelling and optimisation using a RSM method

A central composite matrix was used in order to optimise the experimental conditions of surface texturing process. Central composite second order design was found to be the most efficient tool in response surface modelling using the smallest possible number of tests that still guaranteed a good accuracy. The number of experiments (2^k+2k+n) comes from three parts which is explained as follows [19–21].

- The 2^k points correspond to a complete factorial design, where k is the number of significant influencing factors (in our case 2^2).
- The 2k points are localised at a λ distance from the central point and form a so-called "star figure" (in our case four points). When the value of $\lambda = 2^{k/4}$, the design is rotatable.
- The n points are added in the centre of experiment in order to assure a constant standard error within experimental domain forming a circle of radius 1 (in our case eight points).

The significant influencing factors have been already discussed in a previous paragraph. The central point value of the pulse energy is set to 4 mJ and further tests were done in order to choose the central point value for the pulse frequency. These experiments were run because all previous results showed that a high frequency value is required for all objective functions. Finally, the chosen central point for the pulse frequency was 11,500 Hz. The variation levels of influencing factors are presented in Table 5. Table 6 shows 16 coded combinations used to form the central composite rotatable design matrix and the objective functions obtained values. The tests were performed randomly.

Table 5
Influencing factors and their levels

Influence factors	Notations	Levels				
		−1.41	−1	0	+1	+1.41
Pulse frequency f (Hz)	x_1	10,090	10,500	11,500	12,500	12,910
Pulse energy E (mJ)	x_2	2.6	3	4	5	5.4

Table 6
Central composite second order design matrix and objective functions' observed values

No. of test	Influence factors		Responses		
	x_1	x_2	MRR (mm^3 min^{-1})	S_a (μm)	C_f (mm^2 min^{-1})
1	−1	−1	1.32	8.48	155.37
2	1	−1	1.53	6.18	247.30
3	−1	1	2.04	5.42	376.87
4	1	1	2.37	4.51	481.72
5	−1.41	0	1.78	7.51	236.52
6	1.41	0	2.03	5.02	403.51
7	0	−1.41	1.27	9.40	135.28
8	0	1.41	2.47	6.15	401.86
9	0	0	1.88	5.34	351.73
10	0	0	1.89	5.31	355.93
11	0	0	1.90	5.57	340.89
12	0	0	1.97	4.51	437.18
13	0	0	1.99	4.53	439.11
14	0	0	1.99	5.09	390.23
15	0	0	1.92	5.15	373.46
16	0	0	1.95	4.97	392.22

3.2.1. Mathematical models developing

Response surface methodology (RSM) model corresponds to a second-order polynomial expressed by Eq. (4):

$$\tilde{y} = b_0 + \sum_{i=1}^{n} b_i x_i + \sum_{i=1}^{n} b_{ii} x_i^2 + \sum_{\substack{i,j=1 \\ i \neq j}}^{n} b_{ij} x_i x_j, \quad (4)$$

where $\tilde{y}$ is the corresponding objective function, x_i the coded values of the ith influencing factor, n the numbers of factors and b_0, b_i, b_{ii}, b_{ij}, are the regression coefficients.

Regression coefficients were calculated using the least-square method [20,21]. Their estimated values are listed in Table 7 for all studied objective functions. For determination of coefficients' significance and the suitability of proposed models, analysis of variance (ANOVA) technique was employed [19–21] for a confidence level of 95% (Table 8).

From the ANOVA analysis, it can be concluded that the linear effects of pulse frequency, pulse energy and the effect of quadratic term of pulse energy have a significant influence on material removal rate ($F_{\text{ratio}} > F_{\alpha;v1;v2}$). The effect of quadratic term of pulse frequency and the effect created by the interaction between frequency and energy have no significant influence on the material removal rate. Using these results, a mathematical model was developed in order to estimate the material removal rates and

Table 7
Estimated values of regression coefficients

Regression coefficient	MRR ($mm^3 min^{-1}$)	S_a (μm)	C_f ($mm^2 min^{-1}$)
b_0	1.94	5.06	385.06
b_1	0.11	−0.79	54.19
b_2	0.41	−1.12	104.28
b_{11}	−0.03	0.41	−27.29
b_{22}	−0.05	1.17	−53.17
b_{12}	0.03	0.45	3.23

Table 8
ANOVA test results

Objective functions	Factors	Sum of square, SS	Degrees of freedom, d.f.	Mean square, MS	F_{ratio}[a]
MRR	x_1	0.100	1	0.100	32.056
	X_2	1.326	1	1.326	425.589
	x_1^2	0.009	1	0.009	2.930
	x_2^2	0.021	1	0.021	6.760
	x_1x_2	0.004	1	0.004	1.156
	Error	0.031	10	0.003	
	Total variance	1.491	15	–	–
S_a	X_1	5.009	1	5.01	21.79
	X_2	9.959	1	9.96	43.32
	x_1^2	1.326	1	1.33	5.77
	x_2^2	10.825	1	10.82	47.09
	x_1x_2	0.801	1	0.80	3.48
	Error	2.299	10	0.23	
	Total variance	30.241	15	–	–
C_f	x_1	23423.17	1	23423.17	20.12
	x_2	86744.01	1	86744.01	74.52
	x_1^2	5906.81	1	5906.81	5.07
	x_2^2	22415.75	1	22415.75	19.26
	x_1x_2	41.73	1	41.73	0.04
	Error	11639.96	10	1164.00	
	Total variance	150240.66	15	–	–

α, confidence level; v_1 et v_2, degrees of freedom for each factor.
[a] $F_{\alpha;v1;v2} = 4.96$ ($\alpha = 0.05$, $v_1 = 1$, $v_2 = 10$).

it can be expressed as follows:

$$MRR = 1.94 + 0.11x_1 + 0.41x_2 - 0.05x_2^2, \quad (5)$$

where x_1 and x_2 represent the coded values of pulse frequency pulse energy, respectively.

Two other objective functions are significantly influenced by all effects of linear and quadratic terms of pulse frequency and energy. The interaction between the factors does not have a significant influence on the surface roughness and composite function. Developed models including the significant factors are expressed as follows:

$$S_a = 5.06 - 0.79x_1 - 1.12x_2 + 0.41x_1^2 + 1.17x_2^2 \quad (6)$$

$$C_f = 386.06 + 54.19x_1 + 104.28x_2 - 27.29x_1^2 - 53.17x_2^2. \quad (7)$$

3.2.2. Adequacy verification of developed models

The adequacy of models is checked using the Fisher *F*-test method. If the calculated value of F_{ratio} is less than the standard tabulated value of $F_{\alpha;v1;v2}$ for a desired confidence level, the model is considered to be adequate within the confidence limit. The standard tabulated value of $F_{\alpha;v1;v2}$ is chosen for a desired confidence level (α) and for a number of degrees of freedom (v_1, v_2) of the developed model. The steps for calculating the degrees of freedom and the F_{ratio} value are described in Refs. [19–21]. Fisher test results are presented in Table 9.

Table 9
Fisher test results

Objective function	Fisher *F*-test values	
	Tabulated	Calculated
MRR	$F_{0.05,5;7} = 3.97$	$F_{ratio} = 3.74$
S_a	$F_{0.05,4;7} = 4.12$	$F_{ratio} = 3.66$
C_f	$F_{0.05,4;7} = 4.12$	$F_{ratio} = 0.34$

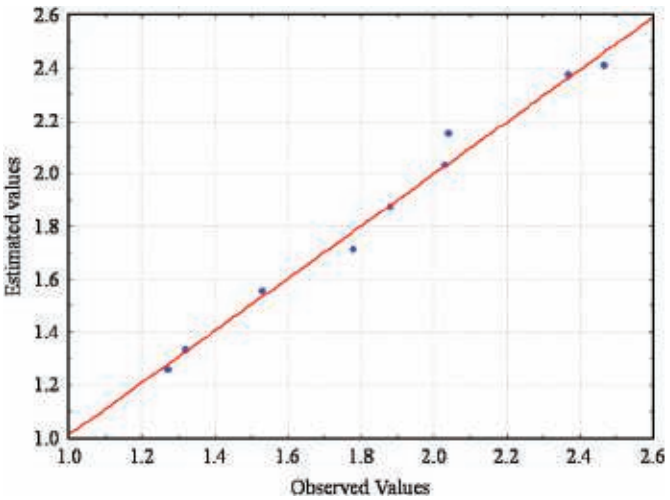

Fig. 6. Estimated vs. observed values of MRR.

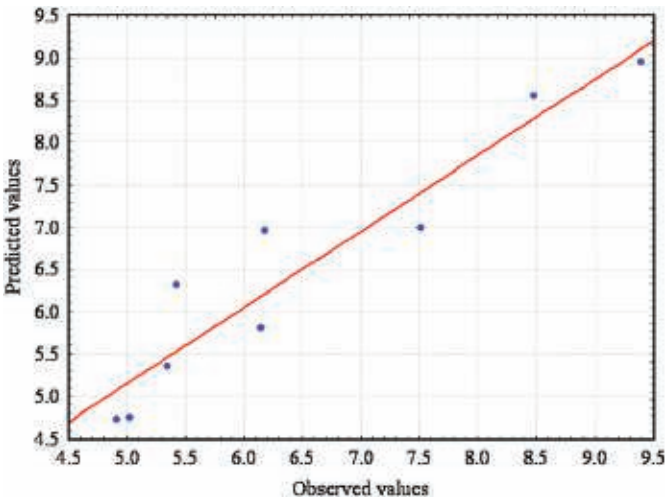

Fig. 7. Estimated vs. observed values of S_a.

According to Fisher test results, it can be concluded that all developed models are adequate for a confidence level of 95%. Despite the simplicity of these models, it is clear that there is a very good agreement between the measured and estimated values (Figs. 6–8), statistically acceptable for a confidence level of 95%. The correlation coefficients (R^2) are calculated using relation (8),

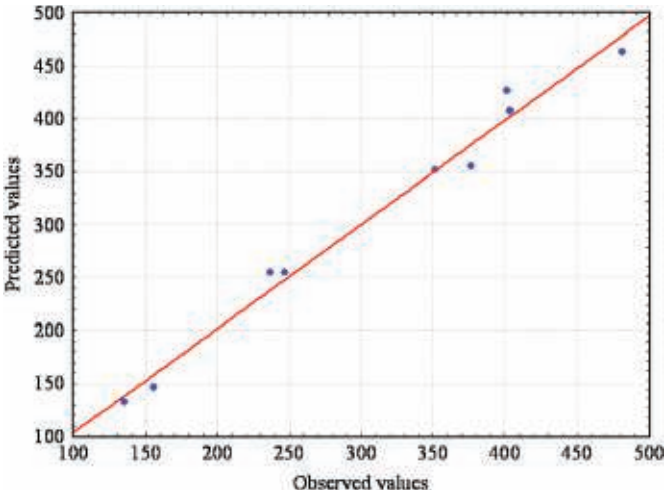

Fig. 8. Estimated vs. observed values of C_f.

and their values are 0.97 for material removal rate, 0.90 for surface roughness and 0.92 for composite function.

$$R^2 = \frac{SS_{\text{total}} - SS_{\text{error}}}{SS_{\text{total}}}. \quad (8)$$

4. Analysis of factors' influence on laser surface texturing process

4.1. Analysis of factors' influences on material removal rate

Analysis of developed mathematical model shows that the pulse energy is the most influential factor on the material removal rate. The combined effects of pulse frequency and pulse energy on the material removal rate are shown in Fig. 9. Material removal rate increases linearly with frequency and pulse energy and decreases linearly when increasing quadratic terms of pulse energy. From a phenomenological point of view, we can say that the material removal rate is controlled by the pulse energy and the pulse duration. In this case, it is possible to assume that the evaporation front propagates with the same speed as the fusion front. This leads to a decrease in time necessary to reach the vaporisation, which as a consequence has an increase in material removal rate. So, the combination of a sufficient energy with a high repetition rate generates a high material removal rate. It can be concluded that, for studied experimental conditions, the maximum of material removal rate can be obtained for a 14 kHz pulse frequency and a 6 mJ pulse energy.

4.2. Analysis of factors' influences on surface roughness

The developed mathematical model shows that the most influential factor on surface roughness is the pulse energy. In the hierarchy of the influencing factors, the first place is taken by the effect of quadratic terms of pulse energy followed by its linear effect. The effects of linear and quadratic terms of pulse frequency are situated on the third and the fourth places, respectively. The combined effects of pulse energy and frequency on surface roughness are plotted in Fig. 10.

The conjunction of an appropriate energy with an acceptable repetition rate is favourable for a good surface roughness. Furthermore, an increase in quadratic terms of these two parameters generates an increase in surface roughness. A good correlation between the pulse energy and the pulse frequency

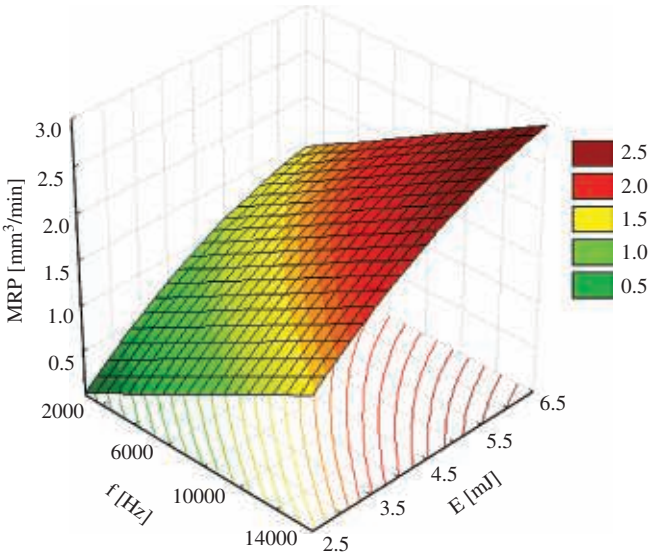

Fig. 9. Response surface for MRR.

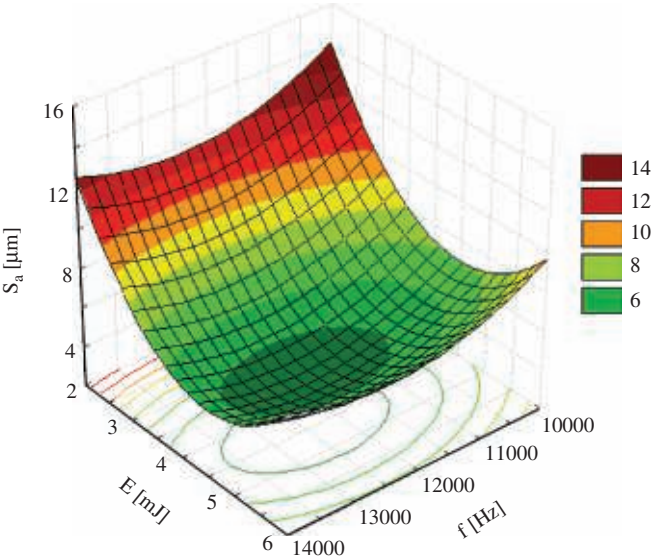

Fig. 10. Response surface for S_a.

generates a reduction of the melted layer thickness. A thin melted layer allows one to obtain a surface less disturbed by the liquid displacement, which occurs under the action of recoil pressure, formed during laser–material interaction. For the studied experimental conditions, the small surface roughness is obtained within the range of 11–14 kHz and 3.5–5.5 mJ, which represents the optimal domain for minimising the surface roughness. The smallest surface roughness (4.5 μm) is obtained for an optimal frequency of 12,500 Hz and an optimal energy of 4.5 mJ.

4.3. Analysis of factors' influences on composite function

Developed mathematical model shows that the composite function is mainly influenced by the pulse energy. The first and second places in the hierarchy of the influencing factors are taken by linear effects of pulse energy and pulse frequency, respectively. The effects of quadratic terms of pulse energy and pulse frequency are situated on the third and the fourth places, respectively.

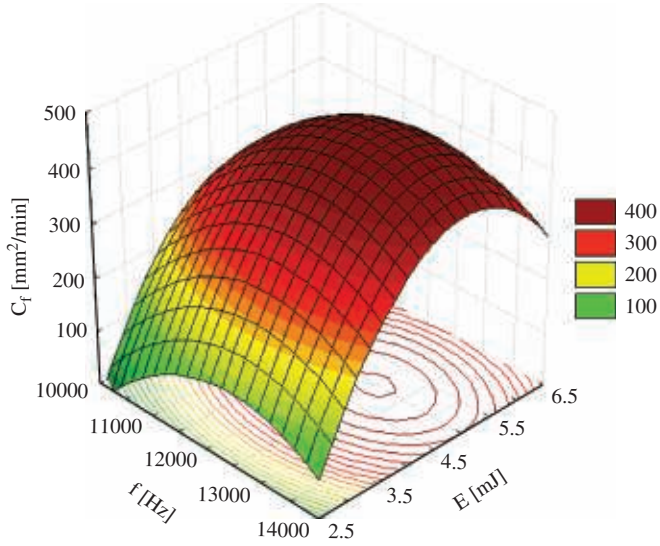

Fig. 11. Response surface for C_f.

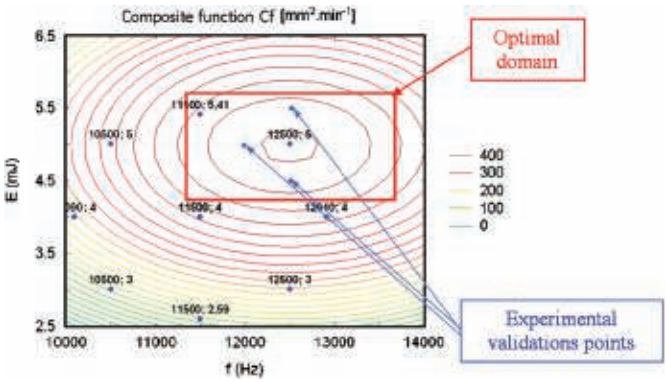

Fig. 12. Optimal working domain.

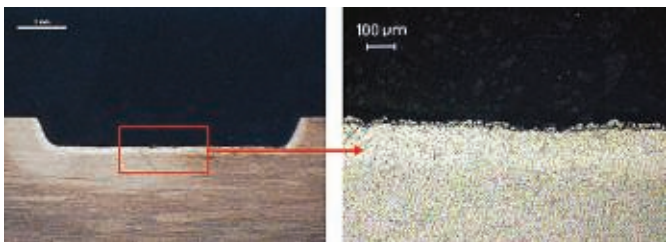

Fig. 13. Optical image of transversal cut of specimen 4.

The composite function value increases with increasing pulse energy and pulse frequency. Further increase in the effects of quadratic terms of these two parameters generates a decrease in composite function. The combined effects of the pulse energy and frequency on the composite function are plotted in Fig. 11.

Within the range of 12–13 kHz and 4.5–5.5 mJ, the variation of composite function is very small. This domain represents the optimal domain for maximising the composite function (Fig. 12). Studied objective function reaches a maximum for a 5 mJ pulse energy and a 12,500 Hz pulse frequency. Since the composite function represents the ratio between the two other studied objective functions, this maximum corresponds to the maximum material removal rate of 2.17 $mm^3\,min^{-1}$ for the smallest surface roughness obtained (4.5 μm, Fig. 13).

5. Conclusions

In this study using an experimental design approach (Taguchi method and RSM method), the factors having a significant influence on studied objective functions were determined. In addition, mathematical modelling of operating parameters influencing the laser surface texturing process was developed. Results analysis shows that only the frequency and energy of pulses, among studied influencing factors, have a significant influence on laser surface texturing process. Material removal rate is directly proportional to linear effects of the pulse energy and frequency, while the surface roughness is inversely proportional to them. Increasing the effects of quadratic terms of pulse energy and frequency generates an increase in surface roughness and decrease in material removal rate. From a phenomenological point of view, it is possible to say that if the liquid layer and its displacement are significant, the pads formation around the impact crater is very significant, as well. This has a negative influence on surface roughness. In this case, in order to minimise the surface roughness, it is necessary to assure the best compromise, which would enable faster reaching of the vaporisation point, reducing the thickness of the melted liquid layer and optimising the covering rate of the impacts. In our case, the optimal set of influencing factors, which enable the maximisation of material removal rate, while preserving a small surface roughness ($S_a < 5\,\mu m$), are a 12.5 kHz pulse frequency and a 5 mJ pulse energy.

The developed models can be used to predict the variation of objective functions with a 95% confidence level, for the range of influencing factors considered in this study investigation. Unfortunately, these models can be used only for those materials which have a similar thermal behaviour under laser irradiation (as other titanium alloys, for example).

This approach allowed us to obtain the best results with a minimum effort (in sense of financial expenses and time) in order to optimise the laser texturing process of titanium alloy.

Comparing the results obtained by laser texturing technique with the other results obtained by other texturing techniques

Table 10
Laser surface texturing compared to other surface texturing methods [22–24]

Texturing technique	Material removal rate	Surface roughness	Observations
Chemical etching	–	$S_a = 4–30\,\mu m$	Etching speed between 0.025 and 0.1 mm min^{-1}
Electro discharge machining EMD	1 $cm^3\,min^{-1}$	$R_a = 10–30\,\mu m$	Only conductors materials
	1–4 $mm^3\,min^{-1}$	$R_a = 0.8–1.6\,\mu m$	
Sand blasting	Low	$R_a = 30\,\mu m$	Low resolution jet
Laser[a]	1–2.3 $mm^3\,min^{-1}$	$S_a = 4–15\,\mu m$	For all materials being opaque to laser beam wavelength

[a] Results obtained in this study.

(Table 10), it is possible to say that the laser beam can successfully be used in order to perform fine surface textures (resembling wood or leather, for example).

Acknowledgements

The authors are very grateful to Prof. Dr. Eng. Alexandru Nichici from the Mechanical Faculty of Timisoara, Romania. His scientific and professional advices in the domain of experimental modelling approaches have been a great support during this study.

References

[1] Almeida IA, de Rossi W, Lima MSF, Beretta JR, Nogueira GEC, Wetter NU, et al. Optimization of titanium cutting by factorial analysis of pulsed Nd:YAG laser parameters. J Mater Process Technol 2006;179:105–10.
[2] Knowles MRH, Rutterford G, Karnakis D, Ferguson A. Laser micromachining of metals, ceramics, silicon and polymers using nanosecond lasers, multi-material micro manufacture (4M), 29–30 June 2005, Karlsruhe, Germany.
[3] Meijer J. Laser beam machining (LBM), state of the art and new opportunities. J Mater Process Technol 2004;149:2–17.
[4] Tuersley IP, Hoult TP, Pashby IR. Nd–YAG laser machining of SiC fibre/borosilicate glass composites. Part I. Optimisation of laser pulse. Compos Part A: Appl Sci Manuf 1998;29:947–54.
[5] Tuersley IP, Hoult TP, Pashby IR. Nd-YAG laser machining of SiC fibre/borosilicate glass composites. Part II. The effect of process variables. Compos Part A: Appl Sci Manuf 1998;29:955–64.
[6] Han A, Grevey D, Nichici A, Pillon G. Study of polymers laser grooving by using the analysis variance method. In: Proceedings of the 24th international congress on application of lasers and electro-optics, 31 October–3 November 2005, Miami, FL, USA
[7] Soveja A, Cicala E, Duffet G, Martin B, Grevey D, Jouvard JM. Empirical modelling of laser texturing of 304L stainless steel. In: Proceedings of the 25th international congress on application of lasers and electro-optics, 30 October–2 November 2006, Scottsdale, AZ, USA
[8] Cicala E, Soveja A, Sallamand P, Grevey D, Jouvard JM. The application of the random balance method in laser machining of metals. J Mater Process Technol 2008;196:393–401.
[9] Lallemand G, Jacrot G, Cicala E, Grevey DF. Grooving by Nd:YAG laser treatment. J Mater Process Technol 2000;99:32–7.
[10] Li Z, Mingjiang Y, Liu W, Zhong M. investigation on crater morphology by high repetitive rate YAG laser-induced discharche texturing. Surf Coat Technol 2006;200:4493–9.
[11] Qi J, Wang KL, Zhu YM. A study on the laser marking process of stainless steel. J Mater Process Technol 2003;139:273–6.
[12] Kaldos A, Pieper HJ, Wolf E, Krause M. Laser machining in die making—a modern rapid tooling process. J Mater Process Technol 2004;155/156:1815–20.
[13] Kuar AS, Doloi B, Bhattacharyya B. Modelling and analysis of pulsed Nd:YAG laser machining characteristics during micro-drilling of Zirconia (ZrO_2). Int J Mach Tools Manuf 2006;46:1301–10.
[14] Du D, He YF, Sui B, Xiong LJ, Zhang H. Laser texturing of rollers by pulsed Nd:YAG laser. J Mater Process Technol 2005;161:456–61.
[15] Yi W, Dang-Sheng X. The effect of laser surface texturing on frictional performance of face seal. J Mater Process Technol 2008;197:96–100
[16] Mirhosseini N, Crouse PL, Schmidth MJJ, Li L, Garrod D. Laser surface micro-texturing of Ti-6Al-4V substrates for improved cell integration. Appl Surf Sci 2007;253:7738–43.
[17] Voevodin AA, Zabinski JS. Laser surface texturing for adaptive solid lubrication. Wear 2006;261:1285–92.
[18] Vigier MG. Pratique des plans d'expériences-méthodologie Taguchi, Les Editions d'Organisation, 1988
[19] Montgomery DC. Design and analysis of experiments. Singapore: Wiley; 1991.
[20] Nichici A, Cicală EF, Mee R. Prelucrarea datelor experimentale-curs și aplicaţii, Litografia Universităţii ''Politehnica,'' Timișoara, 1996
[21] Cicală EF. Metode de prelucrare statistica a datelor experimentale, Ed. Politehnica, Timisoara, 1999.
[22] Arino I, Kleist U, Barros GG, Johansson P, Rigdahl M. Surface texture characterisation of injection-molded pigmented plastics. Polym Eng Sci 2004;44:1615–26.
[23] Balasubramaniam R, Krishnan J, Ramakrishnan N. A study on the shape of the surface generated by abrasive jet machining. J Mater Process Technol 2002;121:102–6.
[24] Kalpakjian S, Schmid SR. Manufacturing processes for engineering materials. 4th ed. Prentice Hall; 2003.